AIAA JOURNAL
Vol. 30, No. 7, July 1992

Control Design Variable Linking for Optimization of Structural/Control Systems

Ik Min Jin* and Lucien A. Schmit†
University of California, Los Angeles, Los Angeles, California 90024

A method is presented to integrate the design space for structural/control system optimization problems in the case of linear state feedback control. Conventional structural sizing variables and elements of the feedback gain matrix are both treated as strictly independent design variables in optimization by extending design variable linking concepts to the control gains. Several approximation concepts, including new control design variable linking schemes, are used to formulate the integrated structural/control optimization problem into a sequence of explicit nonlinear mathematical programming problems. Examples involving a variety of dynamic behavior constraints, including constraints on dynamic stability, control effort, peak transient displacement, acceleration, and control force limits, are effectively solved by using the method presented.

I. Introduction

THERE has been a considerable effort to integrate the design optimization of structures and control systems to handle cross-coupling effects and dynamic interactions between the two systems. Most of this research has focused on linear control laws based on output feedback or state feedback. In the case of output feedback, several studies have been made where the structural dimensions and the control gains are treated as strictly independent design variables in optimization.[1-4] On the other hand, in the case of full-state feedback control, a sequential approach is usually adopted in which the control gains are determined by solving Riccati equations corresponding to the changing structural system during design iterations.[5-8] When the gain variables are determined by solving Riccati equations for a fixed plant, they implicitly become dependent design variables and the resulting design optimization is constrained to a subspace where the optimality conditions of a control subproblem are satisfied. The tendency to subordinate gains to a dependent variable status can be attributed to the fact that for system models with a large number of degrees of freedom, the feedback gain matrix $[H]$ contains prohibitively large numbers of independent design variables (i.e., $M \times 2N$ control design variables, where M is the number of actuators and N is the number of degrees of freedom in the system model).

The method presented here, which is based on Ref. 9, treats both the structural cross-sectional dimensions (CSDs) and elements of the state feedback gain matrix simultaneously as strictly independent design variables during optimization. Design space integration is achieved while using relatively small numbers of control system design variables. This is accomplished by extending design variable linking concepts to the control system gains.

II. Problem Statement

The simultaneous structural/control optimization problem is formulated as a general nonlinear inequality constrained mathematical programming problem as follows:

Find Y to minimize

$$F(Y)$$

Subject to

$$G_j(Y) \le 0, \qquad j = 1, \ldots, NCON \tag{1}$$

With bounds

$$Y_i^L \le Y_i \le Y_i^U, \qquad i = 1, \ldots, NDV$$

where NDV is the total number of design variables, $Y = [Y_1, Y_2, \ldots, Y_{NDV}]^T$ is an $NDV \times 1$ design variable vector, F is a scalar objective function, G_j is the jth behavior constraint, $NCON$ is the total number of behavior constraints, and Y_i^L, Y_i^U are side constraints on the ith design variable.

Both structural and control design variables are included independently in the design variable vector Y. The total mass of the system has been chosen as the objective function and constraints on 1) dynamic stability (real parts of closed-loop eigenvalues), 2) damped frequencies (imaginary parts of closed-loop eigenvalues), 3) peak transient responses, 4) peak transient control forces, and 5) control effort are included in this study.

III. Structural/Control System Description

The second-order equations of motion are

$$[M]\{\ddot{q}\} + [C]\{\dot{q}\} + [K]\{q\} = [b]\{u\} + [e]\{f\} \tag{2}$$

where $\{q\}$ is an $N \times 1$ vector of nodal degrees of freedom (DOF); $\{\dot{q}\}$ and $\{\ddot{q}\}$ are first- and second-time derivatives of $\{q\}$; $[M]$, $[K]$, and $[C]$ are $N \times N$ mass, stiffness, and damping matrices, respectively; $\{u\}$ is an $M \times 1$ actuator force vector, M is the number of actuators; $\{f\}$ is an $L \times 1$ vector of external disturbances, L is the number of external disturbances making up a single load condition; and $[b]$ and $[e]$ are $N \times M$ and $N \times L$ coefficient matrices consisting of the directional cosines that relate actuator and disturbance forces to the nodal DOFs, respectively.

It is assumed that the preassigned damping inherent to the structure can be represented by a proportional damping matrix that is a linear combination of the structural mass and stiffness matrices, i.e.,

$$[C] = c_M[M] + c_K[K] \tag{3}$$

where c_M and c_K are constants.

Presented as Paper 91-1157 at the AIAA/ASME/ASCE/AHS 32nd Structures, Structural Dynamics, and Materials Conference, Baltimore, MD, April 8-10, 1991, received July 1, 1991; revision received Nov. 11, 1991; accepted for publication Nov. 18, 1991.

*Postdoctoral Research Associate, Mechanical, Aerospace, and Nuclear Engineering, 4532 Boelter Hall. Member AIAA.

†Rockwell Professor of Aerospace Engineering, Emeritus, 4531K Boelter Hall. Fellow AIAA.

Equation (2) can be transformed into the first-order state space equation as follows:

$$\{\dot{x}\} = [A_0]\{x\} + [B]\{u\} + [E]\{f\} \tag{4}$$

where

$$\{x\}^T = \lfloor \{q\}^T \{\dot{q}\}^T \rfloor$$

$$[A_0] = \begin{bmatrix} [0] & [I] \\ -[M]^{-1}[K] & -[M]^{-1}[C] \end{bmatrix}$$

$$[B] = \begin{bmatrix} [0] \\ [M]^{-1}[b] \end{bmatrix}$$

$$[E] = \begin{bmatrix} [0] \\ [M]^{-1}[e] \end{bmatrix}$$

The control input vector $\{u\}$ is to be determined under the assumption that all of the states (components of $\{x\}$) are available, that is,

$$\{u\} = -[H]\{x\} = -\left[[H_p][H_v]\right]\begin{Bmatrix} q \\ \dot{q} \end{Bmatrix} \tag{5}$$

where $[H]$ is the $M \times 2N$ feedback gain matrix, and $[H_p]$ and $[H_v]$ are the $M \times N$ position and velocity parts of $[H]$, respectively. The closed-loop equation becomes

$$\{\dot{x}\} = [A]\{x\} + [E]\{f\} \tag{6}$$

where the closed-loop system matrix $[A]$ is

$$[A] = [A_0] - [B][H] =$$

$$\begin{bmatrix} [0] & [I] \\ -[M]^{-1}([K] + [b][H_p]) & -[M]^{-1}([C] + [b][H_v]) \end{bmatrix}$$

IV. Control Design Variable Linking and Initial Controller Design

The main ideas underlying the creation of alternative control design variable linking schemes are 1) separation of velocity and position parts of the gain matrix, 2) various row and column schemes corresponding to actuator and degree of freedom linking, and 3) linking schemes based on only allowing changes in various sets of velocity gains. Combining the forgoing ideas leads to numerous linking schemes with distinct sets and various numbers of independent control system design variables (CDV), ranging from 1 to $M \times 2N$ (see Table 1).

For example, consider option number 5 in Table 1. The feedback gain matrix can be written as follows:

$$[H] = \begin{bmatrix} \lfloor H_p \rfloor_1 & \lfloor H_v \rfloor_1 \\ \lfloor H_p \rfloor_2 & \lfloor H_v \rfloor_2 \\ \cdot & \cdot \\ \cdot & \cdot \\ \cdot & \cdot \\ \lfloor H_p \rfloor_M & \lfloor H_v \rfloor_M \end{bmatrix} = \begin{bmatrix} \alpha_1 \lfloor H_p^0 \rfloor_1 & \alpha_{M+1} \lfloor H_v^0 \rfloor_1 \\ \alpha_2 \lfloor H_p^0 \rfloor_2 & \alpha_{M+2} \lfloor H_v^0 \rfloor_2 \\ \cdot & \cdot \\ \cdot & \cdot \\ \cdot & \cdot \\ \alpha_M \lfloor H_p^0 \rfloor_M & \alpha_{2M} \lfloor H_v^0 \rfloor_M \end{bmatrix} \tag{7}$$

The left-hand side represents the $M \times 2N$ feedback gain matrix in partitioned row-wise form ($\lfloor H_p \rfloor_j$, $\lfloor H_v \rfloor_j$ represent jth rows of $[H_p]$ and $[H_v]$, respectively), and the right-hand side has participation coefficients (α_i) in front of the partitioned rows of the initial startup gain matrix before the linking scheme is imposed (superscript 0 denotes the initial startup matrix). During optimization, the various α_i are treated as independent design variables (simultaneously with the CSDs), and as they are optimized, the feedback gain matrix $[H]$ is optimized in the constrained design space in accordance with the fixed ratios established by the rows of the initial startup matrix.

Table 1 Control design variable linking options

Option	Description	Design variables	No. of independent CDVs
1	Totally unlinked	Elements of $[H]$	$M \times 2N$
2	$[H_p]$ fixed, $[H_v]$ unlinked	Elements of $[H_v]$	$M \times N$
3	Columns of $[H]$ linked	Coefficients of columns of $[H]$	$2N$
4	$[H_p]$ fixed, columns of $[H_v]$ linked	Coefficients of columns of $[H_v]$	N
5	Rows of $[H_p]$ and $[H_v]$ linked	Coefficients of rows of $[H_p]$ and $[H_v]$	$2M$
6	Rows of $[H]$ linked	Coefficients of rows of $[H]$	M
7	$[H_p]$ fixed, rows of $[H_v]$ linked	Coefficients of rows of $[H_v]$	M
8	$[H_p]$, $[H_v]$ linked	Coefficients of $[H_p]$, $[H_v]$	2
9	$[H_p]$ fixed, $[H_v]$ linked	Coefficient of $[H_v]$	1
10	$[H]$ linked	Coefficient of $[H]$	1

When a specific control design variable linking scheme is used, it is important to choose an acceptable set of initial startup feedback gains because the relative values of certain elements in the feedback gain matrix remain frozen throughout the design process according to the linking scheme selected. Three different methods for generating the initial startup gain matrix are suggested.

The first initializing method sets the feedback gains arbitrarily (e.g., $[H] = [0]$) and then carries out a few design iterations without control design variable linking of any kind. This allows all of the gains as well as the structural design variables to change freely for a few iterations to find a reasonable initial design before imposing some linking on the set of $M \times 2N$ control design variables. Even though the unlinked option is used for only a few iterations, this can still be a serious restriction, limiting the application of the method to small problems.

The second method is to solve the $2N \times 2N$ nonlinear matrix Riccati equation once to find the linear optimal control law corresponding to the initial structural design. The initial gain values obtained from the matrix Riccati equation solution are then used as startup gains to establish fixed ratios between the gains that are assumed to hold throughout the design optimization process.

The third method is the decoupled Riccati equation solution scheme, which gives an approximate solution to the full-order Riccati equation. This method uses normal modes to diagonalize the original equations of motion, and then for each second-order scalar equation a linear quadratic regulator (LQR) problem is solved, neglecting the coupling effects.

The second and third initializing methods are described further in the following sections.

Full-Order Riccati Equation

Consider Eqs. (2) and (4) with the external disturbance terms set to zero (i.e., $\{f\} = \{0\}$):

$$[M]\{\ddot{q}\} + [C]\{\dot{q}\} + [K]\{q\} = [b]\{u\} \tag{8}$$

$$\{\dot{x}\} = [A_0]\{x\} + [B]\{u\} \tag{9}$$

The optimal control law to minimize a given performance index

$$PI = \int_0^\infty \left(\{x\}^T[Q]\{x\} + \{u\}^T[R]\{u\} \right) dt \tag{10}$$

where $[Q]$ and $[R]$ are $2N \times 2N$ positive semidefinite and $M \times M$ positive definite weighting matrices for states and control forces, respectively, can be determined from

$$\{u\} = -[H]\{x\} = -[R]^{-1}[B]^T[P]\{x\} \tag{11}$$

where the $2N \times 2N$ positive semidefinite symmetric matrix $[P]$ satisfies the following matrix Riccati equation:

$$[P][A_0] + [A_0]^T[P] + [Q] - [P][B][R]^{-1}[B]^T[P] = [0] \tag{12}$$

Decoupled Riccati Equation Solution

An alternative method that bypasses solution of the full-order Riccati equation is presented. First find the natural frequencies and normal modes of

$$[M]\{\ddot{q}\} + [K]\{q\} = \{0\} \tag{13}$$

that is, solve the standard eigenproblem

$$\omega_i^2[M]\{v_i\} = [K]\{v_i\}, \qquad i = 1, 2, \ldots, r \tag{14}$$

and normalize the modes $\{v_i\}$ so that

$$\{v_i\}^T[M]\{v_j\} = \delta_{ij}, \qquad i,j = 1, 2, \ldots, r \tag{15}$$

where δ_{ij} is the Kronecker delta, and r is the number of normal modes to be used in the decoupled Riccati equation solution ($r \le N$). Note that r should be at least equal to or greater than the number of structural modes to be controlled. Let

$$\{q\} = [V]\{z\} \tag{16}$$

where the ith column of the $N \times r$ normal mode matrix $[V]$ is the ith normal mode $\{v_i\}$, and $\{z\} = \lfloor z_1, z_2, \ldots, z_r \rfloor^T$ is an $r \times 1$ normal coordinate vector. Substituting Eq. (16) into Eq. (8) and premultiplying by $[V]^T$ results in r sets of scalar equations as follows:

$$\ddot{z}_i + c_i\dot{z}_i + \omega_i^2 z_i = \{v_i\}^T[b]\{u\}$$

$$= \{v_i\}^T[b]\left(\{u\}^{(i)} + \sum_{k \ne i}^{r} \{u\}^{(k)}\right) \tag{17}$$

where

$$\{u\}^{(i)} = -\left[\{\tilde{H}_p\}^{(i)}\{\tilde{H}_v\}^{(i)}\right]\begin{Bmatrix} z_i \\ \dot{z}_i \end{Bmatrix}, \qquad i = 1, 2, \ldots, r \tag{18}$$

The vector $\{u\}^{(i)}$ is an $M \times 1$ control vector that contains only ith normal mode components (z_i and $\dot{z}_i$). Furthermore, $\{\tilde{H}_p\}^{(i)}$ and $\{\tilde{H}_v\}^{(i)}$ are $M \times 1$ feedback gain vectors that relate $\{u\}^{(i)}$ with z_i, $\dot{z}_i$, respectively. It is noted that $c_i = c_M + c_K\omega_i^2$, in view of the proportional damping assumption embodied in Eq. (3).

Now assume that the ith control vector $\{u\}^{(i)}$ can be calculated independently, neglecting the coupling term [second term on the right-hand side of Eq. (17)], and that the resulting $\{u\}$ is the sum of all of the $\{u\}^{(i)}$, i.e.,

$$\{u\} = \sum_{i=1}^{r} \{u\}^{(i)} = -\left[[\tilde{H}_p][\tilde{H}_v]\right]\begin{Bmatrix} z \\ \dot{z} \end{Bmatrix} \tag{19}$$

where $[\tilde{H}_p]$ and $[\tilde{H}_v]$ denote $M \times r$ position and velocity gain matrices in normal coordinates, the columns of which are $\{\tilde{H}_p\}^{(i)}$ and $\{\tilde{H}_v\}^{(i)}$, respectively. Then using the relation $\{z\} = [V]^T[M]\{q\}$, the feedback gain matrix in physical coordinates can be recovered as follows:

$$[H_p] = [\tilde{H}_p][V]^T[M], \qquad [H_v] = [\tilde{H}_v][V]^T[M] \tag{20}$$

Now the remaining problem consists of finding r sets of $\{u\}^{(i)}$. Neglecting the coupling terms in Eq. (17) yields

$$\ddot{z}_i + c_i\dot{z}_i + \omega_i^2 z_i \cong \{v_i\}^T[b]\{u\}^{(i)} \tag{21}$$

which can be transformed into the standard first-order state space form, so that

$$\{\dot{w}_i\} = [A_i]\{w_i\} + [B_i]\{u\}^{(i)}$$

$$[A_i] = \begin{bmatrix} 0 & 1 \\ -\omega_i^2 & -c_i \end{bmatrix}, \qquad [B_i] = \begin{bmatrix} [0] \\ \{v_i\}^T[b] \end{bmatrix} \tag{22}$$

where $\{w_i\} = \lfloor z_i \ \dot{z}_i \rfloor^T$ is the 2×1 state vector, $[A_i]$ the 2×2 system open-loop matrix, and $[B_i]$ the $2 \times M$ system input matrix for the ith modal equation.

The performance index for the ith mode (PI_i) is chosen as

$$PI_i = \int_0^\infty \left(\{w_i\}^T[Q_i]\{w_i\} + \{u\}^{(i)T}[R_i]\{u\}^{(i)} \right) dt \tag{23}$$

where $[Q_i] = \text{Diag}\,[Q_{11}^i, Q_{22}^i] (Q_{11}^i, Q_{22}^i > 0)$ is a 2×2 diagnonal weighting matrix for the ith state vector and $[R_i] = \gamma_i[I]$ ($[I]$ is an $M \times M$ identity matrix, $\gamma_i > 0$) is a weighting matrix for the ith modal control force vector. Then the ith component of the control $\{u\}^{(i)}$ can be determined by

$$\{u\}^{(i)} = -[R_i]^{-1}[B_i]^T[P_i]\{w_i\} \tag{24}$$

where the 2×2 positive semidefinite symmetric matrix

$$[P_i] = \begin{bmatrix} p_{11}^i & p_{12}^i \\ p_{12}^i & p_{22}^i \end{bmatrix}$$

satisfies the 2×2 Riccati equation

$$[P_i][A_i] + [A_i]^T[P_i] + [Q_i] - [P_i][B_i][R_i]^{-1}[B_i]^T[P_i] = [0] \tag{25}$$

Equation (25) can be solved in closed form, and the results are

$$p_{12}^i = p_{21}^i = \frac{-\omega_i^2 + \sqrt{\omega_i^4 + W_iQ_{11}^i}}{W_i}$$

$$p_{22}^i = \frac{-c_i + \sqrt{c_i^2 + W_iQ_{22}^i - 2\omega_i^2 + 2\sqrt{\omega_i^4 + W_iQ_{11}^i}}}{W_i} \tag{26}$$

$$p_{11}^i = c_ip_{12}^i + \omega_i^2 p_{22}^i + p_{12}^i p_{22}^i W_i$$

where

$$W_i = \{v_i\}^T[b][R_i]^{-1}[b]^T\{v_i\} = \frac{1}{\gamma_i}\{v_i\}^T[b][b]^T\{v_i\} \tag{27}$$

By comparing Eq. (18) and Eq. (24), the ith feedback gain vectors in normal coordinates can be obtained as follows:

$$\{\tilde{H}_p\}^{(i)} = \frac{p_{12}^i}{\gamma_i}[b]^T\{v_i\}, \qquad \{\tilde{H}_v\}^{(i)} = \frac{p_{22}^i}{\gamma_i}[b]^T\{v_i\} \tag{28}$$

Substituting Eq. (24) into Eq. (21) yields, after some manipulation,

$$\ddot{z}_i + (c_i + W_ip_{22}^i)\dot{z}_i + (\omega_i^2 + W_ip_{12}^i)z_i \cong 0 \tag{29}$$

To summarize, the original full-order Riccati equation is replaced by r sets of 2×2 Riccati equation [Eq. (25)] that have

explicit closed-form solutions [Eq. (26)]. Then the feedback gain matrix $[\tilde{H}] = [[\tilde{H}_p][\tilde{H}_v]]$ in normal coordinates is transformed to $[H]$ in the original coordinate system by using normal mode information.

The method presented in this section has a considerable advantage over the full-order Riccati equation solution approach. It is, in fact, explicit and efficient enough to permit periodic updating of the initial fixed ratios between elements of the gain matrix $[H]$. When the fixed ratios of the feedback gain matrix are updated, special attention is given to preserving continuity of the real part of the closed-loop eigenvalues, so that the dynamic behavior remains relatively smooth between the updating stages (see the Appendix).

V. Analysis

Complex Eigenproblem

Since the closed-loop $[A]$ matrix [see Eq. (6)] is not symmetric, eigenvalues and eigenvectors are complex, and two distinct sets of eigenvectors exist for each eigenvalue. For the ith eigenvalue λ_i, the right eigenvector $\{\phi_i\}$ and the left-hand eigenvector $\{\psi_i\}$ satisfy

$$[A]\{\phi_i\} = \lambda_i\{\phi_i\}, \qquad \{\psi_i\}^T[A] = \lambda_i\{\psi_i\}^T \tag{30}$$

These two sets of eigenvectors are normalized such that[10]

$$\{\phi_i\}^T\{\phi_i\} = d_i, \qquad \{\psi_i\}^T\{\phi_i\} = \delta_{ij} \tag{31}$$

where d_i is a normalizing scalar constant for the ith right eigenvector and δ_{ij} is a Kronecker delta.

Dynamic Transient Response

Time-dependent response and control force constraints are replaced with a finite number of peak value constraints by first finding the corresponding peak times using the adaptive one-dimensional method described in Ref. 11.

To calculate the transient response of a given system, Eq. (6) should be integrated in the time domain. Since Eq. (6) is coupled and usually large, a set of complex eigenvectors is chosen as a basis to diagonalize and reduce the dimensions of the original equation. Let

$$\{x\} = [\Phi]\{\eta\} \tag{32}$$

where $[\Phi]$ is a $2N \times 2R (R \leq N)$ right-hand eigenmatrix and $\{\eta\}$ is a $2R \times 1$ complex normal coordinate vector and $2R$ is the number of complex modes (out of $2N$) that are retained to calculate truncated responses. Substituting Eq. (32) into Eq. (6) and premultiplying by $[\Psi]^T$ ($2R \times 2N$ left-hand eigenmatrix transposed) yields

$$\{\dot{\eta}\} = [\Lambda]\{\eta\} + [\Psi]^T[E]\{f\} \tag{33}$$

Equation (33) is equivalent to the following set of $2R$ first-order scalar differential equations

$$\dot{\eta}_i = \lambda_i\eta_i + \{\psi_i\}^T[E]\{f\}, \qquad i = 1, 2, \ldots, 2R \tag{34}$$

Integrating Eq. (34) with respect to time gives

$$\eta_i(t) = e^{\lambda_i(t-t_0)}\eta_i(t_0) + \int_{t_0}^{t} e^{\lambda_i(t-\tau)}\{\psi_i\}^T[E]\{f(\tau)\}\, d\tau \tag{35}$$

where t_0 is an initial time and t is a specific time of interest. Here $\{f(t)\}$ is assumed to be expressed in terms of a truncated Fourier series and polynomials over a specified period of time, i.e.,

$$\{f(t)\} = \sum_{k=1}^{N_\Omega}(\{FC\}_k \cos \Omega_k t + \{FS\}_k \sin \Omega_k t) + \sum_{p=0}^{N_p}\{FP\}_p t^p \qquad \text{when } 0 \leq t \leq t_f$$
$$\{f(t)\} = 0 \qquad \text{when } t > t_f \tag{36}$$

where t_f is the specified time interval during which disturbances are applied, N_Ω is the number of different driving frequencies, $\{FC\}_k$ and $\{FS\}_k$ are $L \times 1$ vectors that contain cosine and sine components corresponding to the kth driving frequency Ω_k, N_p denotes the highest order polynomial term considered, and the $L \times 1$ vector $\{FP\}_p$ corresponds to the pth-order polynomial. Then Eq. (35) has a closed-form solution. After calculating the various η_i, the state vector $\{x(t)\}$ can be recovered from Eq. (32) and the control force vector $\{u(t)\}$ from Eq. (5).

Control Effort

Assuming the control effort contribution during the time interval $0 \leq t \leq t_f$ is negligibly small compared with that during the time period $t_f \leq t < \infty$, control effort is given by

$$CE = \int_{t_f}^{\infty}\{u\}^T[R_{CE}]\{u\}\, dt = \int_{t_f}^{\infty}\{x\}^T[Q_{CE}]\{x\}\, dt \tag{37}$$

where t_f is the time interval during which the external disturbance force is applied, $[R_{CE}]$ is an $M \times M$ positive definite symmetric weighting matrix, and $[Q_{CE}] = [H]^T[R_{CE}][H]$.

Substituting Eq. (32) into Eq. (37) gives

$$CE = \int_{t_f}^{\infty}\{\eta\}^T[\Phi]^T[Q_{CE}][\Phi]\{\eta\}\, dt = \int_{t_f}^{\infty}\{\eta\}^T[\tilde{Q}]\{\eta\}\, dt \tag{38}$$

where $[\tilde{Q}] = [\Phi]^T[Q_{CE}][\Phi]$. Then the control effort is given by

$$CE = \{\eta(t_f)\}^T[\tilde{W}]\{\eta(t_f)\} \tag{39}$$

where $[\tilde{W}]$ satisfies

$$[\Lambda][\tilde{W}] + [\tilde{W}][\Lambda] = -[\tilde{Q}] \tag{40}$$

which is a Lyapunov equation. Equation (40) can be solved element by element leading to

$$\tilde{W}_{ij} = -\frac{\tilde{Q}_{ij}}{\lambda_i + \lambda_j} \tag{41}$$

where $\tilde{W}_{ij}$ and $\tilde{Q}_{ij}$ are the i,jth element of $[\tilde{W}]$ and $[\tilde{Q}]$, respectively ($\tilde{Q}_{ij} = \{\phi_i\}^T[Q_{CE}]\{\phi_j\}$).

VI. Sensitivity Analysis

To generate approximate design optimization problems, first-order system sensitivity information with respect to both structural and control design variables is required. Derivatives of $[H]$ with respect to control design variables are obtained directly and derivatives of $[M]$, $[C]$, and $[K]$ with respect to structural variables are obtained analytically from the finite-element formulation. From this information, analytic sensitivities of the system $[A]$ and $[E]$ matrices [see Eq. (6)] can be obtained with respect to an arbitrary intermediate or direct design variable α. Since it is assumed that the external loads are expressed in terms of a truncated Fourier series and polynomials over a specified period of time, it is possible to calculate all of the (first-order) behavior sensitivity derivatives analytically.

Eigenproblem Sensitivities

Eigenvalue sensitivities ($\partial\lambda_i/\partial\alpha$) are needed not only because eigenvalues themselves can be behavior constraints but also because they are required to calculate other response sensitivities. Furthermore, to obtain precise transient response sensitivities, eigenvector sensitivities ($\partial[\Phi]/\partial\alpha$ and $\partial[\Psi]/\partial\alpha$) are also calculated using an analytic method.[12]

Transient Response Sensitivities

For an arbitrary peak time t, peak response sensitivities can be calculated by differentiating Eq. (32) as

$$\frac{\partial\{x(t)\}}{\partial\alpha} = \frac{\partial[\Phi]}{\partial\alpha}\{\eta(t)\} + [\Phi]\frac{\partial\{\eta(t)\}}{\partial\alpha} \tag{42}$$

In the previous equation, the only term not previously discussed is $\partial\{\eta(t)\}/\partial\alpha$, and it can be obtained by differentiating Eq. (35) with respect to the design variable α, assuming that the external disturbances are independent of the design variables, i.e., Ω_k, $\{FC\}_k$, $\{FS\}_k$, $k = 1, N_\Omega$ and $\{FP\}_p$, $p = 1, N_p$ are constant. It should be noted that the previous calculation is only carried out at previously identified peak response or peak control force times.

Control Effort Sensitivity

The sensitivity of the control effort is obtained by differentiating Eq. (39),

$$\frac{\partial(CE)}{\partial\alpha} = \{\eta(t_f)\}^T \frac{\partial[\tilde{W}]}{\partial\alpha}\{\eta(t_f)\} + 2\{\eta(t_f)\}^T[\tilde{W}]\frac{\partial\{\eta(t_f)\}}{\partial\alpha} \tag{43}$$

In the previous expression, the only unknown term is $\partial[\tilde{W}]/\partial\alpha$, and it can be determined by differentiating Eq. (41) as follows:

$$\frac{\partial\tilde{W}_{ij}}{\partial\alpha} = \frac{1}{(\lambda_i+\lambda_j)^2}\left(\frac{\partial\lambda_i}{\partial\alpha}+\frac{\partial\lambda_j}{\partial\alpha}\right)\tilde{Q}_{ij} - \frac{1}{(\lambda_i+\lambda_j)}\frac{\partial\tilde{Q}_{ij}}{\partial\alpha} \tag{44}$$

where

$$\frac{\partial\tilde{Q}_{ij}}{\partial\alpha} = \{\phi_i\}^T\frac{\partial[Q_{CE}]}{\partial\alpha}\{\phi_j\} + \frac{\partial\{\phi_i\}^T}{\partial\alpha}[Q_{CE}]\{\phi_j\} + \{\phi_i\}^T[Q_{CE}]\frac{\partial\{\phi_j\}}{\partial\alpha} \tag{45}$$

VII. Optimization—Approximate Problems

Various approximation concepts such as structural and control design variable linking, temporary constraint deletion, and intermediate design variables[13,14] are used to replace the original design optimization problem by a series of explicit approximate problems. Linear, reciprocal, or hybrid approximations can be generated with respect to either direct or intermediate design variables, even though the approximate design optimization problems are always solved in an integrated design space that spans the actual structural CSDs and the participation coefficients of the linked control gains. Each approximate optimization problem has its own lower and upper bounds on the design variables. These bounds are determined by the move limits or the original side constraints [see Eq. (1)], whichever is most restrictive. For frame elements it is known that the section properties A, I_y, I_z, and J are good choices for intermediate design variables. This follows from the fact that the elements of the stiffness and the mass matrices are linear functions of these section properties. Control design variables are used directly in the generation of the approximate problem because the system matrices are linear functions of the gains.

With the information acquired from the analysis and sensitivity analysis phase, each approximate optimization problem can be formulated as follows:

Find Y to minimize

$$\tilde{F}[X(Y)]$$

Subject to

$$\tilde{G}_j[X(Y)] \le 0, \qquad j \in Q_R \tag{46}$$

With bounds

$$\underline{Y}_i \le Y_i \le \bar{Y}_i, \qquad i = 1, \ldots, NDV$$

where NDV is the total number of design variables, Y is a vector of design variables ($NDV \times 1$), $NIDV$ is the total number of intermediate design variables, $X(Y)$ is a vector of intermediate design variables ($NIDV \times 1$), $\tilde{F}(\cdot)$ is an approximate objective function, $\tilde{G}_j(\cdot)$ is the jth approximate constraint, $\underline{Y}_i$ and $\bar{Y}_i$ are lower and upper bounds of the ith design variable (during solution of the current approximate optimization problem), and Q_R is the retained set of constraints for the current approximate problem. For all of the numerical examples presented in this paper, the following approximation options are employed. Linear approximation of $\tilde{F}(\cdot)$ is used with respect to intermediate structural design variables (A, I_y, I_z, J), which is exact when the mass is minimized. When generating the approximate constraint functions, linear approximation is chosen with respect to control design variables whereas the hybrid approximation is used with respect to structural intermediate design variables.

VIII. Numerical Results

The control augmented structural optimization solution method described in the previous sections has been implemented on the IBM 3090 mainframe computer at UCLA. CONMIN[15] is used as the optimizer. Numerical results that illustrate the effectiveness of alternative control design variable linking schemes are presented here.

Antenna Structure

An antenna structure is chosen as the example to be presented here. Numerical results for other example problems can be found in Ref. 9. It consists of eight aluminium beams ($E = 7.3 \times 10^6$ N/cm^2, $\rho = 2.77 \times 10^{-3}$ kg/cm^3, $\nu = 0.325$) that have thin-walled hollow box beam cross sections (see Fig. 1). This structure is constrained to move vertically (Y direction) only, so each nodal point has 3 degrees of freedom (translation in the Y direction and rotation about the X and Z reference axes shown in Fig. 1) resulting in the total of 18 degrees of freedom ($N = 18$). Four translational actuators ($M = 4$) weighing 4 kg each are attached to nodes 3, 5, 6, and 7. These actuators are oriented so that the force they generate acts in the vertical direction (degrees of freedom 4, 10, 13, and 16). Two ramp-type transient loads are applied to node 3 at the same time. One is a vertical force $[f_1(t)]$ and the other is a moment $[f_2(t)]$ about a line parallel to the X reference axis but passing through node 3 that gives antisymmetric exitation. These loads are given as follows:

$$f_1(t) = 333.3t \text{ N}, \qquad f_2(t) = 10.0 \times [f_1(t)] \text{ N} \cdot \text{cm}$$

for $0 \le t \le 0.3$ s, and $f_1(t) = f_2(t) = 0$ for $t > 0.3$ s (see Fig. 1). Transient response is considered for the time interval $0 \le t \le 2$ s

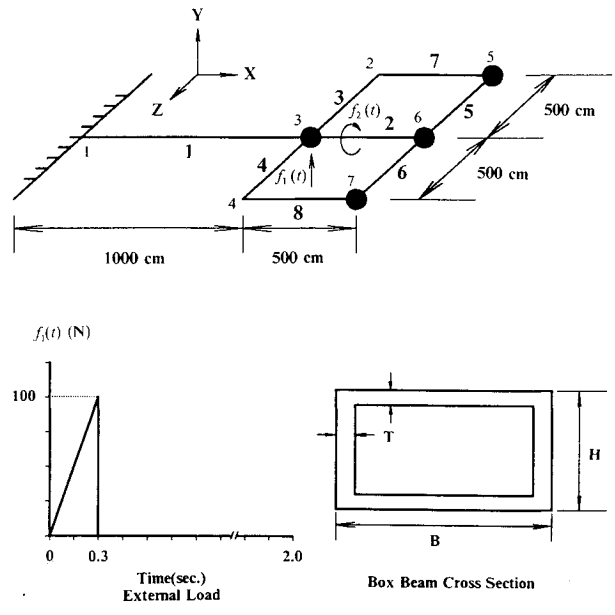

Fig. 1 Antenna structure.

and 20 out of 36 complex modes ($2R = 20$) are used to calculate the peak response values. Passive damping is assumed to be zero ($c_M = c_K = 0$). This assumption tends to be conservative for transient response constraints, and it is further justified by observing that the magnitude of damping inherent to the structural system is likely to be small compared with that introduced by an active control system.

The design objective to be minimized is the total mass of the system including the fixed actuator masses as well as the variable structural mass. Flange and web thicknesses are constrained to be the same, so there are three structural design variables for each finite element (B, H, and T). Structural linking is also used to make the structure remain symmetric with respect to the XY plane, which results in the total of 15 independent structural design variables. The initial structure is uniform ($B = H = 20.0$ cm, $T = 0.5$ cm), and the side constraints are 10.0 cm $\leq B, H \leq 25.0$ cm, and 0.1 cm $\leq T \leq 1.0$ cm. The maximum number of control design variables is relatively large ($M \times 2N = 144$).

Move limits of 30% for both structural variables and control variables are used, unless otherwise mentioned. In all cases, behavior constraints are imposed on 1) the real part of all of the retained complex modes ($\sigma_i \leq -0.5$); 2) the fourth and fifth damped frequencies ($\omega_{d4} \geq 8.0$ Hz, $\omega_{d5} \geq 9.25$ Hz); 3) the peak displacement of nodes 2, 4, 5, and 7 ($|q_i(t)| \leq 1.0$ cm, $i = 1, 7, 10$, and 16); and 4) the peak actuator force ($|u_j(t)| \leq 8.5$ N, $j = 1, 2, 3$, and 4). In cases 14 and 15, additional constraints are imposed on the control effort and the peak acceleration, respectively. For the decoupled Riccati equations, the 2×2 state weighting matrices are set to be $[Q_i] = \text{Diag}\,[\omega_i^2, 1]$, $i = 1, 2, \ldots, r$ so that the first term of Eq. (23) represents a total (strain and kinetic) modal energy, and the control weighting coefficients γ_i are chosen to be 1/400. In Fig. 2, the initial closed-loop eigenvalues obtained by solving 10 sets ($r = 10$) of 2×2 Riccati equations are compared with those obtained from a full-order Riccati equation solution, and as can be seen from the plot, these two solution methods give almost the same values for the lowest 10 modes.

Cases 1-10, Control Design Variable Linking

Cases 1-10 correspond to 10 different control design variable linking schemes. Initial startup gains are computed by solving 10 sets of 2×2 Riccati equations ($r = 10$) and the 10 distinct control design variable linking schemes listed in Table 1 are imposed from the beginning. Iteration histories are shown in Table 2 and final structural designs in Table 3. Design masses include the fixed actuator masses as well as the variable structural mass.

Table 2 Iteration histories for antenna example: cases 1-10

	Total mass, kg									
Analysis	Case 1	Case 2	Case 3	Case 4	Case 5	Case 6	Case 7	Case 8	Case 9	Case 10
1	502.14	502.14	502.14	502.14	502.14	502.14	502.14	502.14	502.14	502.14
2	462.20	462.39	466.52	462.25	455.96	469.64	465.14	485.24	474.45	484.61
3	345.34	343.47	349.71	351.13	359.45	367.65	361.18	383.18	374.55	387.64
4	254.17	259.92	261.19	263.19	283.10	293.90	280.72	302.66	291.97	297.69
5	213.91	218.31	235.33	230.47	231.57	237.33	231.87	241.31	234.26	240.14
6	184.11	191.87	210.26	213.59	212.83	218.09	212.22	216.56	214.15	215.05
7	174.34	176.98	199.19	200.50	204.21	205.11	204.82	208.12	207.01	208.60
8	168.93	170.94	192.61	195.82	200.82	201.28	201.05	206.07	207.00	206.33
9	169.35	167.01	193.88	194.60	198.91	200.51	200.69	205.78	204.60	206.07
10	165.61	166.99	190.74	192.95	198.71	200.35	200.63	204.22	204.47	206.06
11	164.42	165.43	188.11	191.28	198.45	200.27	200.59	204.19	204.46	206.06
12	164.08	165.03	185.03	189.94	198.01			204.16		
13	164.17	164.84	185.75	189.03	197.42					
14	163.99	164.64	184.26	187.51	196.93					
15	163.76	164.39	182.27	186.92	196.46					
16	163.20	164.19	180.79	186.66	196.32					
17	163.10	164.10	179.90	186.50	196.31					
18	163.11	164.05	179.79	186.34						
19			179.64							
Option[a]	1	2	3	4	5	6	7	8	9	10
CDVs[b]	144	72	36	18	8	4	4	2	1	1

[a]Control design variable linking option number. [b]Number of independent CDVs.

Table 3 Final designs for antenna example: cases 1-10

	Cross-sectional dimensions, cm										
Case	Element 1	Element 2	Element 3,4	Element 5,6	Element 7,8	Case	Element 1	Element 2	Element 3,4	Element 5,6	Element 7,8
B	25.00[b]	25.00[b]	23.24	25.00[b]	19.31		25.00[b]	25.00[b]	22.04	25.00[b]	10.84
H 1	25.00[b]	25.00[b]	25.00[b]	25.00[b]	25.00[b]	6	25.00[b]	25.00[b]	25.00[b]	25.00[b]	24.83
T	0.1000[a]	0.1108	0.1000[a]	0.1935	0.1000[a]		0.2166	0.1496	0.1000[a]	0.2134	0.1000[a]
B	25.00[b]	25.00[b]	24.11	25.00[b]	18.68		25.00[b]	25.00[b]	20.95	25.00[b]	12.08
H 2	25.00[b]	25.00[b]	25.00[b]	25.00[b]	24.99	7	25.00[b]	25.00[b]	25.00[b]	25.00[b]	24.86
T	0.1046	0.1129	0.1000[a]	0.1908	0.1000[a]		0.2054	0.1360	0.1000[a]	0.2323	0.1000[a]
B	25.00[b]	25.00[b]	17.68	25.00[b]	18.87		25.00[b]	25.00[b]	19.04	25.00[b]	14.43
H 3	25.00[b]	25.00[b]	24.41	25.00[b]	25.00[b]	8	25.00[b]	25.00[b]	25.00[b]	25.00[b]	25.00[b]
T	0.1393	0.1263	0.1000[a]	0.2202	0.1000[a]		0.1790	0.1115	0.1000[a]	0.2832	0.1000[a]
B	25.00[b]	25.00[b]	16.67	25.00[b]	18.56		25.00[b]	25.00[b]	18.47	25.00[b]	14.50
H 4	25.00[b]	25.00[b]	21.92	25.00[b]	25.00[b]	9	25.00[b]	25.00[b]	25.00[b]	25.00[b]	25.00[b]
T	0.1454	0.1213	0.1000[a]	0.2490	0.1000[a]		0.1752	0.1129	0.1000[a]	0.2883	0.1000[a]
B	25.00[b]	25.00[b]	21.55	25.00[b]	13.82		25.00[b]	25.00[b]	19.13	25.00[b]	15.80
H 5	25.00[b]	25.00[b]	25.00[b]	25.00[b]	25.00[b]	10	25.00[b]	25.00[b]	25.00[b]	25.00[b]	25.00[b]
T	0.1748	0.1152	0.1000[a]	0.2526	0.1000[a]		0.1904	0.1000[a]	0.1000[a]	0.2815	0.1000[a]

[a]Indicates lower bound value. [b]Indicates upper bound value.

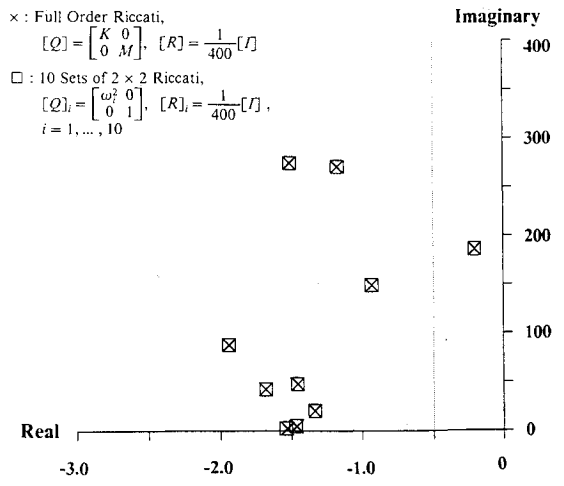

Fig. 2 Comparison of initial closed-loop eigenvalues.

As the freedom in the design space is reduced by imposing more restrictive control design variable linking schemes (from case 1 to 10), it can be clearly seen from the results that 1) the number of independent control variables in the optimization loop decreases (from 144 to 1), 2) the optimum mass increases (from 163.11 to 206.06 kg), and 3) total number of iterations decreases and the convergence becomes more robust.

It is important to note that even with only one independent control design variable, the final objective mass value obtained (206.06 kg, case 10) is 14.8% lower than the result reported in Ref. 5 (241.97 kg). This can be attributed to the fact that in Ref. 5 the control gains are not independent design variables since, for any particular set of structural design variables, they are determined from the solution of an LQR subproblem.

Even though there is more than 20% of difference in the optimum mass between case 1 and 10, all cases show a similar trend in the final structural design. Namely, widths and depths of finite elements 1, 2, 5, and 6 take on their upper bound values and thicknesses of elements 3, 4, 7, and 8 move to their lower bound values (see Table 3).

In the following sections, additional cases are investigated and their results are presented in Tables 4 and 5.

Cases 11 and 12, Arbitrary Initial Gains

This section examines the first method for initializing the startup control gain matrix before imposing control variables linking. In cases 11 and 12 two different sets of initial gains are chosen and four iterations are allowed without any control design variable linking (number of CDVs = 144). The results of the unlinked iterations are then used as initial startup gains and the last linking option is imposed (number of CDV = 1). In case 11, the initial gains are the same as in cases 1-10 (obtained by solving 10 sets of decoupled Riccati equations). In case 12 the initial gain matrix is chosen in a manner similar to that which would be used if direct output feedback control was being employed [$H(1, 4) = H(2,10) = H(3,13) = H(4,16) = 500$ kg/s^2, $H(1,22) = H(2,28) = H(3,31) = H(4,34) = 500$ kg/s, $H(j,i) = 0$, elsewhere]. In case 12 large move limits are used for small feedback gain elements (190% or absolute value of 100) to give more freedom at the beginning.

Case 13, Updating Fixed Ratios in Gain Matrices

Case 13 is identical to case 10 except that the feedback gain matrix is re-solved at the beginning of each iteration to update the fixed ratios in the gain matrix. After 10 updating stages, all of the coefficients of the control force weighting matrix [γ_i, see Eq. (23)] converge within 3%.

Table 4 Iteration histories for antenna example: cases 11-15

	Total mass, kg				
Analysis	Case 11	Case 12	Case 13	Case 14	Case 15
1	502.14	502.14	502.14	502.14	502.14
2	462.20	527.16	484.61	479.30	490.26
3	345.34	544.29	385.71	401.68	383.79
4	254.17	461.82	287.94	336.30	327.58
5	213.91	399.83	239.17	288.54	308.81
6	184.11	346.49	211.97	266.27	300.07
7	174.34	309.54	203.64	254.49	294.66
8	172.94	276.72	201.39	249.05	290.57
9	174.24	245.00	201.29	247.92	285.01
10	174.18	225.77	201.03	246.37	284.93
11	174.18	207.78	201.00	245.93	284.71
12		202.86	200.99	245.44	
13		201.34		245.17	
14		200.61		245.01	
15		199.42		245.01	
16		199.42			
17		199.42			

Table 5 Final designs for antenna example: cases 11-15

		Cross-sectional dimensions, cm				
	Case	Element 1	Element 2	Element 3,4	Element 5,6	Element 7,8
B		25.00[b]	25.00[b]	20.21	25.00[b]	17.10
H	11	25.00[b]	24.90[b]	25.00[b]	25.00[b]	23.99[b]
T		0.1124	0.1572	0.1000[a]	0.2112	0.1000[a]
B		25.00[b]	25.00[b]	25.00[b]	25.00[b]	12.45
H	12	25.00[b]	25.00[b]	25.00[b]	21.11	25.00[b]
T		0.2032	0.1921	0.1000[a]	0.2092	0.1000[a]
B		25.00[b]	25.00[b]	20.36	25.00[b]	15.71
H	13	25.00[b]	25.00[b]	25.00[b]	25.00[b]	25.00[b]
T		0.1736	0.1000[a]	0.1000[a]	0.2774	0.1000[a]
B		25.00[b]	25.00[b]	15.89	25.00[b]	17.92
H	14	25.00[b]	25.00[b]	25.00[b]	23.50	21.21
T		0.3567	0.1779	0.1000[a]	0.2370	0.1000[a]
B		25.00[b]	25.00[b]	25.00	25.00[b]	25.00[b]
H	15	19.59	24.92	25.00[b]	21.94	22.49
T		0.3728	0.2706	0.2401	0.1550	0.1347

[a]Indicates lower bound value. [b]Indicates upper bound value.

Cases 14 and 15, Additional Behavior Constraints

Case 14 is identical to case 10 except for an additional constraint that is imposed on the control effort (CE ≤ 20 N$^2 \cdot$ s). The 4×4 control weighting matrix [R_{CE}] is chosen to be an identity matrix [see Eq. (37)].

Case 15 is identical to case 10 except that in this case additional constraints are imposed on the accelerations of nodes 2, 4, 5, and 7 ($|a_k(t)| \leq 100$ cm/s^2, $k = 1$, 7, 10, and 16).

Summary and Discussion

In all cases, damped frequency, peak response, and peak control force constraints are active. Cases 1-10 investigate the effect of linking schemes on the convergence characteristics and the minimum mass achieved. Generally, as more linking is imposed, the final mass increases and the design converges faster and more smoothly. In Fig. 3, final masses are compared with the number of independent control variables according to the distinct control design variable linking options chosen.

Between cases 11 and 12, case 11 shows lower optimum mass and better convergence than case 12. This shows that even when the first method for obtaining the startup gain matrix is used, it is important to choose some meaningful initial gains. For this example, starting from the initial gains obtained by solving a set of 2×2 Riccati equations gives much better results. Cases 11-13 give final structural designs similar to cases 1-10 (i.e., widths and depths of finite elements 1, 2, 5, and 6 take on their upper bound values, and thicknesses of

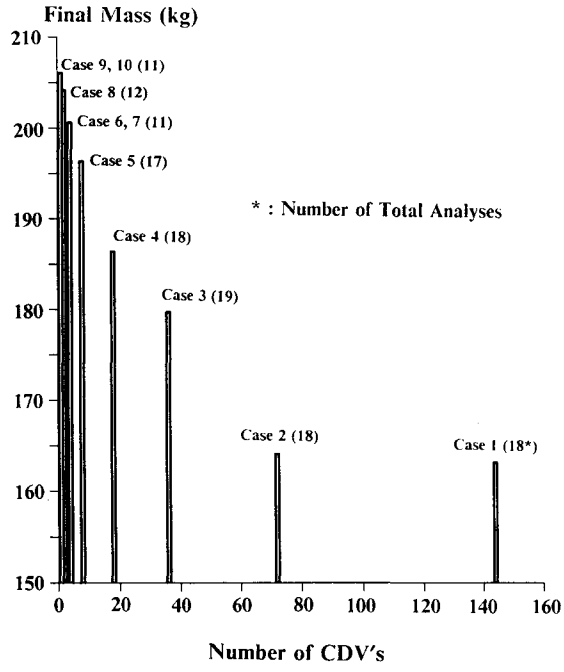

Fig. 3 Number of CDVs vs final mass: antenna structures, different CDV linkings.

elements 3, 4, 7, and 8 move to their lower bound values). On the other hand, cases 14 and 15, where control effort and acceleration constraints are imposed, exhibit a different type of structural design with a larger mass (especially case 15, see Table 5), that can be attributed primarily to the presence of additional behavior constraints.

IX. Conclusion

It is shown that the design variable linking concept can be extended to control system design variables. In the context of full-state feedback control, design variable linking makes it possible to treat structural design variables (SDVs) and control design variables (CDVs) simultaneously without having to deal with prohibitively large numbers of design variables. Furthermore, the 2×2 decoupled Riccati equation solution method makes it possible to obtain good startup values for the elements of the gain matrix $[H] = [[H_p]\ [H_v]]$, without the computational burden of having to solve a full-order ($2N \times 2N$) Riccati equation. The method presented shows promise in the sense that it offers the prospect of being able to exploit the benefits of full-state feedback and true integration without having to 1) repeatedly solve large $2N \times 2N$ Riccati equations or 2) deal with extremely large numbers of independent design variables.

Acknowledgment

This research was supported by NASA Research Grant NSG 1490.

Appendix: Updating Fixed Ratios of Control Gains

As mentioned in the text, imposing some kind of linking on the feedback gains fixes the relative values of those elements through the final stage. When the approximate decoupled Riccati equation solution is used, this condition can be relaxed. When the 2×2 Riccati equations are solved again for a changing structure, there should be some rule to choose weighting matrices $[Q_i]$ and $[R_i]$ of Eq. (23). Since the real parts of the eigenvalues (σ_i) have a strong influence on the dynamic response and are also directly constrained, the scheme presented here has focused on preserving continuity of the σ_i during the re-solution of the feedback gain matrix.

From Eq. (29) the closed-loop eigenvalue of the ith equation λ_i satisfies

$$\lambda_i^2 + (c_i + W_i p_{22}^i)\lambda_i + (\omega_i^2 + W_i p_{12}^i) \cong 0 \tag{A1}$$

from which (assuming underdamped motion)

$$\lambda_i = \sigma_i \pm j\omega_{d_i} \tag{A2}$$

where

$$\sigma_i = \frac{-(c_i + W_i p_{22}^i)}{2}$$

$$\omega_{d_i} = \frac{\sqrt{4(\omega_i^2 + W_i p_{12}^i) - (c_i + W_i p_{22}^i)^2}}{2}$$

From the previous derivation noting that $\{v_i\}$, $[b]$, ω_i^2, and c_i are fixed for a given structure, the complex eigenvalues λ_i can be assigned arbitrarily by adjusting W_i, p_{12}^i, and p_{22}^i or equivalently γ_i, Q_{11}^i, and Q_{22}^i [see Eqs. (26) and (27)].

The ratio between the state weighting matrix $[Q_i] = \text{Diag}\,[Q_{11}^i, Q_{22}^i]$ and the control weighting matrix $[R_i] = \gamma_i [I]$ determines the relative magnitude of states and control forces. This means that the ratio between $[Q_i]$ and $[R_i]$ (or Q_{11}^i, Q_{22}^i, and γ_i) will determine the damping effect in the ith mode, so by changing only γ_i the real part of the closed-loop eigenvalue can be assigned (within some bounds).

The forgoing observations suggest that for some iterations (for example for every K iterations) the fixed ratios within the feedback gain matrix can be updated by changing the γ_i in a manner that forces the real part of the closed-loop eigenvalues to coincide with the approximate real part of the eigenvalues (σ_i) from the previous iteration, i.e., from Eq. (A2) and the expression for p_{22}^i

$$\tilde{\sigma}_i = -\frac{(c_i + W_i p_{22}^i)}{2} = -\tfrac{1}{2}\sqrt{c_i^2 + W_i Q_{22}^i - 2\omega_i^2 + 2\sqrt{\omega_i^4 + W_i Q_{11}^i}} \tag{A3}$$

or

$$W_i = \frac{1}{(Q_{22}^i)^2}(X + 2Q_{11}^i - 2Y) \tag{A4}$$

where

$$Y = \sqrt{Q_{11}^i X + (Q_{22}^i)^2 + \omega_i^4 (Q_{22}^i)^2}$$

$$X = Q_{22}^i(4\tilde{\sigma}_i^2 + 2\omega_i^2 - c_i^2)$$

Then from Eq. (27)

$$\gamma_i = \frac{1}{W_i}\{v_i\}^T[b][b]^T\{v_i\} \tag{A5}$$

With a new set of γ_i the decoupled Riccati equations are solved again so that the relative values of the elements in the gain matrix are updated according to the changing structure while preserving continuity of the real parts of the complex eigenvalues between the iterations. When all of the γ_i converge to the previous values, this updating option can be turned off.

References

[1]Lust, R. V., and Schmit, L. A., "Control Augmented Structural Synthesis," NASA CR 4132, April 1988.

[2]Thomas, H. L., and Schmit, L. A., "Improved Approximations for Control Augmented Structural Synthesis," *Proceedings of the AIAA/ASCE/ASCE/AHS/ASC Structures, Structural Dynamics, and Materials Conference,* Pt. I, AIAA, Washington, DC, 1990, pp. 277–294.

[3]Junkins, J. L., and Rew, D. W., "Unified Optimization of Structures and Controllers," *Large Space Structures: Dynamics and Control,* edited by S. N. Atluri and A. K. Amos, Springer-Verlag, Berlin, 1988, pp. 323–353.

[4]McLaren, M. D., and Slater, G. L., "A Covariance Approach to Integrated Control/Structure Optimization," *Proceedings of the AIAA Dynamics Specialist Conference,* AIAA Paper 90-1211, AIAA, Washington, DC, 1990, pp. 189-205.

[5]Sepulveda, A. E., and Schmit, L. A., "Optimal Placement of Actuators and Sensors in Control Augmented Structural Optimization," *International Journal for Numerical Methods in Engineering,* Vol. 32, No. 6, 1991, pp. 1165-1187.

[6]Khot, N. S., Venkayya, V. B., and Eastep, F. E., "Optimal Structural Modifications to Enhance the Active Vibration Control of Flexible Structures," *AIAA Journal,* Vol. 24, No. 8, 1986, pp. 1368-1374.

[7]Miller, D. F., and Shim, J., "Gradient-Based Combined Structural and Control Optimization," *Journal of Guidance, Control, and Dynamics,* Vol. 10, No. 3, 1987, pp. 291-298.

[8]Grandhi, R. V., "Structural and Control Optimization of Space Structures," *Computers and Structures,* Vol. 31, No. 2, 1989, pp. 139-150.

[9]Jin, I. M., "Control Design Variable Linking for Optimization of Structural/Control Systems," Ph.D. Dissertation, Univ. of California, Los Angeles, Dept. of Mechanical, Aerospace, and Nuclear Engineering, Los Angeles, CA, 1991.

[10]Lim, K. B., Junkins, J. L., and Wang, B. P., "Re-Examination of Eigenvector Derivatives," *Journal of Guidance, Control, and Dynamics,* Vol. 10, No. 6, 1987, pp. 581-587.

[11]Grandhi, R. V., Haftka, R. T., and Watson, L. T., "Design-Oriented Identification of Critical Times in Transient Response," *AIAA Journal,* Vol. 24, No. 4, 1986, pp. 649-656.

[12]Nelson, R. B., "Simplified Calculation of Eigenvector Derivatives," *AIAA Journal,* Vol. 14, No. 9, pp. 1201-1205.

[13]Schmit, L. A., and Farshi, B., "Some Approximation Concepts for Efficient Structural Synthesis," *AIAA Journal,* Vol. 12, No. 5, 1974, pp. 692-699.

[14]Schmit, L. A., and Miura, H., "Approximation Concepts for Efficient Structural Synthesis," NASA CR 2552, March 1976.

[15]Vanderplaats, G. N., "CONMIN—A Fortran Program for Constrained Function Minimization," NASA TM X-62,682, Aug. 1973.